J Electroceram (2011) 26:105–111
DOI 10.1007/s10832-011-9636-9

Normal sintering and electric properties of (K,Na,Li)(Nb,Sb)O_3 lead-free piezoelectric ceramics

Lei Zhang · Jianxing Shen · Jiaoxian Yu · Hongshi Zhao · Zhiliang Xiu · Chunlei Yan · Chuanshan Li · Jinmei Dong · Yuan Ma

Received: 19 December 2007 / Accepted: 28 February 2011 / Published online: 23 March 2011

Abstract $0.94(K_{05}Na_{0.5})NbO_3-0.03LiNbO_3-0.03LiSbO_3$ (KNLNS) lead-free piezoelectric ceramics were prepared by conventional mixed oxide route with normal sintering method. The samples were sintered at different temperatures with KNLNS powder atmosphere to prevent volatilization of alkali metal oxides at high temperature. The effects of sintering temperature on the density, structure and electric properties of KNLNS ceramics were studied. X-ray diffraction (XRD) results showed that the crystal structure of the crushed KNLNS ceramic powders were pure perovskite phase with tetragonal phase structure when sintered at $T \leq 1080°C$. However a $K_3Li_2Nb_5O_{15}$ phase with tetragonal tungsten bronze structure began to appear when the sintering temperature was higher than 1080°C. The optimum sintering temperature was 1080°C which was determined by measuring the density of the samples. Scanning electron microscope (SEM) observation indicated that the sintering temperature had a great effect on the microstructure of the samples. The KNLNS ceramics under the optimum sintering temperature showed excellent electric properties: $\rho=4.29$ g/cm^3, $\varepsilon_r=826$, $\tan\delta=0.049$, $d_{33}=190$ pC/N, $k_p=0.30$, and $T_c=385°C$. The results show that the KNLNS ceramics are promising candidate for lead-free piezoelectric ceramics.

L. Zhang · J. Shen (✉) · J. Yu · H. Zhao · Z. Xiu · C. Yan · C. Li · J. Dong · Y. Ma
Key Laboratory of Processing and Testing Technology of Glass & Functional Ceramics of Shandong Province, Department of Materials Science and Engineering, Shandong Polytechnic University, Jinan 250353, P.R. China
e-mail: sjx@sdili.edu.cn

L. Zhang · J. Yu · Z. Xiu · Y. Ma
State Key Lab of Crystal Materials, Shandong University, Jinan 250100, P.R. China

Keywords Lead-free piezoelectric ceramics · Sintering · Piezoelectric properties

1 Introduction

Piezoelectric ceramics have been widely used for sensors, ultrasonic transducers, actuators and other electronic devices [1, 2]. Most of them are lead oxide-based piezoelectric ceramics, which contain more than 60 wt.% lead [3]. Lead zirconate titanate (Pb(Zr,Ti)O_3, abbreviated as PZT) ceramics are playing a dominant role in piezoelectric materials due to their superior piezoelectric properties. However lead is a very toxic substance, and the evaporation and contamination of toxic lead during the fabrication and disposal can cause a crucial environmental pollution. Therefore, it is necessary and urgent to develop lead-free piezoelectric ceramics to replace lead-based piezoelectric ceramics. Nowadays, the researches on lead-free piezoelectric ceramics mainly focus on bismuth titanates and alkali noibates, and system in which a morphotropic phase boundary (MPB) occurs. Among them, $(Na_{0.5}K_{0.5})NbO_3$ (NKN) has been considered as a good candidate for lead-free piezoelectric ceramics due to its good piezoelectric properties [4, 5]. The hot pressed NKN ceramics has been reported to possess high Curie temperature ($T_c=420°C$), large piezoelectric constant ($d_{33}=160$ pC/N) and high planar coupling coefficients ($k_p=0.45$) [6]. However, NKN is difficult to densify by conventional sintering technique because of high volatilization of Na_2O and K_2O at high temperature. Hot pressing, hot isostatic pression and spark plasma sintering have been used to achieve high density [7–9]. But the cost is relatively high and the size of piezoelectric material is limited. From the industrial point of view, these methods are not suitable for mass production. According to the phase diagram of the $KNbO_3$–$NaNbO_3$

system, there exists a liquid and solid region with a solidus point of about 1140°C at the equal mole composition [10]. The normal sintering of KNN ceramics is required to be conducted at temperatures at least above 1060°C, which is actually extremely high if considering the above-mentioned solidus point. Therefore, in this paper, a crucible together with powder atmosphere was adopted to prevent volatilization of alkali metal oxides at high temperature.

Recently, most researchers have investigated the effects of small amount of dopants into NKN ceramics such as $SrTiO_3$[11], $BaTiO_3$[12], $CaTiO_3$[13], $LiNbO_3$[14], $LiTaO_3$[15], $LiSbO_3$[16] to improve densification and piezoelectric properties. Among these NKN-based systems, (1-x)$(Na_{0.5}K_{0.5})NbO_3$−x$LiNbO_3$, (1−x)$(Na_{0.5}K_{0.5})NbO_3$−x$LiTaO_3$ and (1−x)$(Na_{0.5}K_{0.5})NbO_3$−x$LiSbO_3$ poses a morphotropic phase boundary (MPB) at x=0.05–0.06, where the system show outstanding piezoelectric and electric properties[14–16]. It is also reported that $(K_{0.48}Na_{0.48}Li_{0.04})(Nb_{0.9}Ta_{0.1})O_3$, $(K_{0.44}Na_{0.52})(Nb_{0.86}Ta_{0.1})O_3$−0.04$LiSbO_3$ solid solution have particularly high piezoelectric properties [17, 18]. However, the price of Ta_2O_5 is very expensive. Adding a great deal of Ta to KNN ceramics will limit the applications of the material. There is little work reporting on both $LiNbO_3$ and $LiSbO_3$ modified NKN ceramics. Therefore, the additions of $LiNbO_3$ and $LiSbO_3$ to $(K_{0.5}Na_{0.5})NbO_3$ are used in this work. It is expected that by adding appropriate amount of $LiNbO_3$ and $LiSbO_3$, enhanced piezoelectric and electric properties will be obtained. From our earlier experiment, optimum performances of NKN ceramic occur as doping 3 mol% $LiNbO_3$ and 3 mol% $LiSbO_3$. Therefore, the composition of 0.94$(K_{0.5}Na_{0.5})NbO_3$−0.03$LiNbO_3$−0.03-$LiSbO_3$ (abbreviated as KNLNS) ceramics were chosen in our work. Most properties of piezoelectric ceramics, such as density, dielectric and piezoelectric properties, strongly

Table 1 The properties comparison of $(K_{05}Na_{0.5})NbO_3$ ceramics based on our present results and other reports published in the literature

Compositions	ρ (g/cm^3)	ε_r	tanδ	d_{33} (pC/N)	k_p	T_c (°C)	Method	Reference
$(Na_{0.5}K_{0.5})NbO_3$	4.46	420	-	160	0.45		HIP	[6]
$(Na_{0.5}K_{0.5})NbO_3$	4.25	290	-	80	0.36		Conv	[6]
$(Na_{0.5}K_{0.5})NbO_3$	4.47	606	0.036	148	0.389	395	SPS	[9]
0.96$(Na_{0.5}K_{0.5})NbO_3$ −0.04$SrTiO_3$	-	1091	0.035	52	0.156	280	CIP	[11]
0.94$(Na_{0.5}K_{0.5})NbO_3$ −0.06$BaTiO_3$	4.44	1003	0.038	104	0.29	358	CIP	[12]
0.94$(Na_{0.5}K_{0.5})NbO_3$ −0.06$LiNbO_3$	4.31	530	0.034	215	0.41	450	Conv	[14]
0.94$(Na_{0.5}K_{0.5})NbO_3$ −0.06$LiTaO_3$	-	570	0.05	200	0.36	430	CIP	[15]
0.995$(Na_{0.5}K_{0.5})NbO_3$ −0.005$CaTiO_3$	4.40	553	-	115	0.379	-	Conv	[13]
0.94$(Na_{0.5}K_{0.5})NbO_3$ −0.06$LiSbO_3$	4.44	708	0.037	171	0.38	365	Conv	[16]
0.935$(Na_{0.5}K_{0.5})NbO_3$ −0.065$LiNbO_3$	4.38	680	0.18	250	0.44	450	Conv	[17]
$(K_{0.48}Na_{0.48}Li_{0.04})$ $(Nb_{0.9}Ta_{0.1})O_3$	4.46	560	0.03	160	0.47	380	Conv	[17]
$(K_{0.44}Na_{0.52})$ $(Nb_{0.86}Ta_{0.1})O_3$−0.04$LiSbO_3$	-	-	-	300	-	-	Conv	[18]
$(K_{0.44}Na_{0.52})$ $(Nb_{0.86}Ta_{0.1})O_3$−0.04$LiSbO_3$	-	1570	-	416	0.61	253	Textured	[18]
0.94$(Na_{0.5}K_{0.5})NbO_3$ −0.03$LiNbO_3$ −0.03$LiSbO_3$	4.29	826	0.049	190	0.30	385	Conv	Our sample

HIP: Hot isostatic pressed
SPS: Spark plasma sintering
CIP: Cold isostatic pressing
Conv: Conventional method

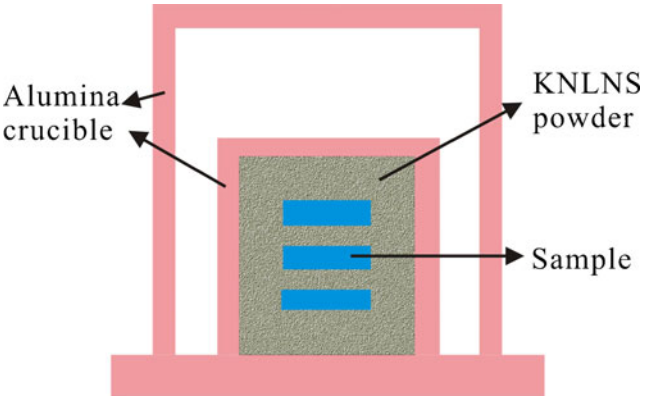

Fig. 1 Schematic illustration of normal sintering with a powder bed

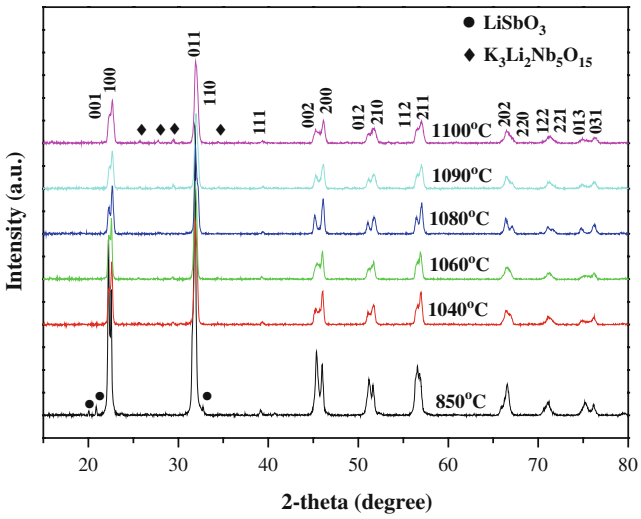

Fig. 2 XRD patterns of $0.94(K_{05}Na_{0.5})NbO_3$–$0.03LiNbO_3$–$0.03LiSbO_3$ crushed ceramic powders sintered at 1040–1100°C and powder samples calcined at 850°C

depend on the sintering temperature. Therefore, it is necessary to investigate the effect of sintering temperature on the structure and properties of KNN-based piezoelectric ceramics. In this paper, $0.94(K_{0.5}Na_{0.5})NbO_3$–$0.03LiNbO_3$–$0.03LiSbO_3$ (abbreviated as KNLNS) ceramics were fabricated by conventional solid state reaction with normal sintering. The optimal normal sintering condition of KNLNS ceramics were determined. The effects of the sintering temperature on the phase structure, microstructure and electrical properties were investigated. The properties comparison of NKN ceramics based on our present results and other reports published in the literature are demonstrated in Table 1. Compared with other NKN-based piezoelectric ceramics, it can be concluded that KNLNS piezoelectric ceramics sintered at 1080°C is a promising candidate for lead-free piezoelectric ceramics.

2 Experimental

The conventional ceramic fabrication technique was used to prepare $0.94(K_{05}Na_{0.5})NbO_3$–$0.03LiNbO_3$–$0.03LiSbO_3$ ceramics. Reagent−grade carbonate and oxide powders of K_2CO_3, Na_2CO_3, Li_2CO_3, Nb_2O_5 and Sb_2O_3 were used as starting materials. The powders of these raw materials were mixed by a planetary milling with zirconia ball media and alcohol for 15 h. The mixed powders were calcined at 850°C for 5 h. Then these powders were ball milled again for 15 h. The milled powders were dried, grinded and granulated with polyvinylalcohol (PVA) binder. The granulated powder was pressed into disks with diameter of 15 mm and thickness of 1 mm. To prevent high volatilization of alkali metal oxides at high temperature during sintering, the pressed disks were covered with powders of the same composition and sintered at 1040–1110°C for 2 h (Fig. 1). Silver paste was painted on both sides of the disks to form electrodes, and then subsequently fired at 750°C for 15 min. Samples for piezoelectric measurements were poled in silicon oil bath at 80°C for 20 min under the electric field of 3 kV/mm.

The density of the sintered samples was measured by the Archimedes method. The phase structure of the calcined powders and crushed ceramic powders was examined using an X-ray diffractometer with Cu$K\alpha$ radiation (D8 Advance, Bruker AXS, Germany). The microstructure was observed using a scanning electron microscope (Quanta200, FEI, Holand). According to the resonance and anti-resonance method, piezoelectric characteristics were measured using an impedance analyzer (Agilent 4294A). The piezoelectric constant d_{33} was measured using a quasistatic d_{33} meter

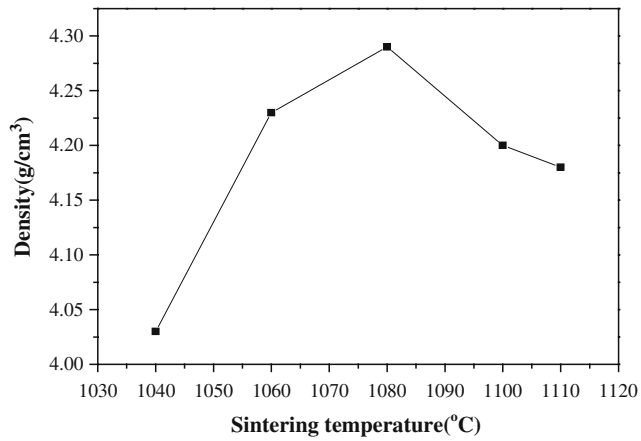

Fig. 3 Density of $0.94(K_{05}Na_{0.5})NbO_3$–$0.03LiNbO_3$–$0.03LiSbO_3$ ceramics sintered at different temperatures

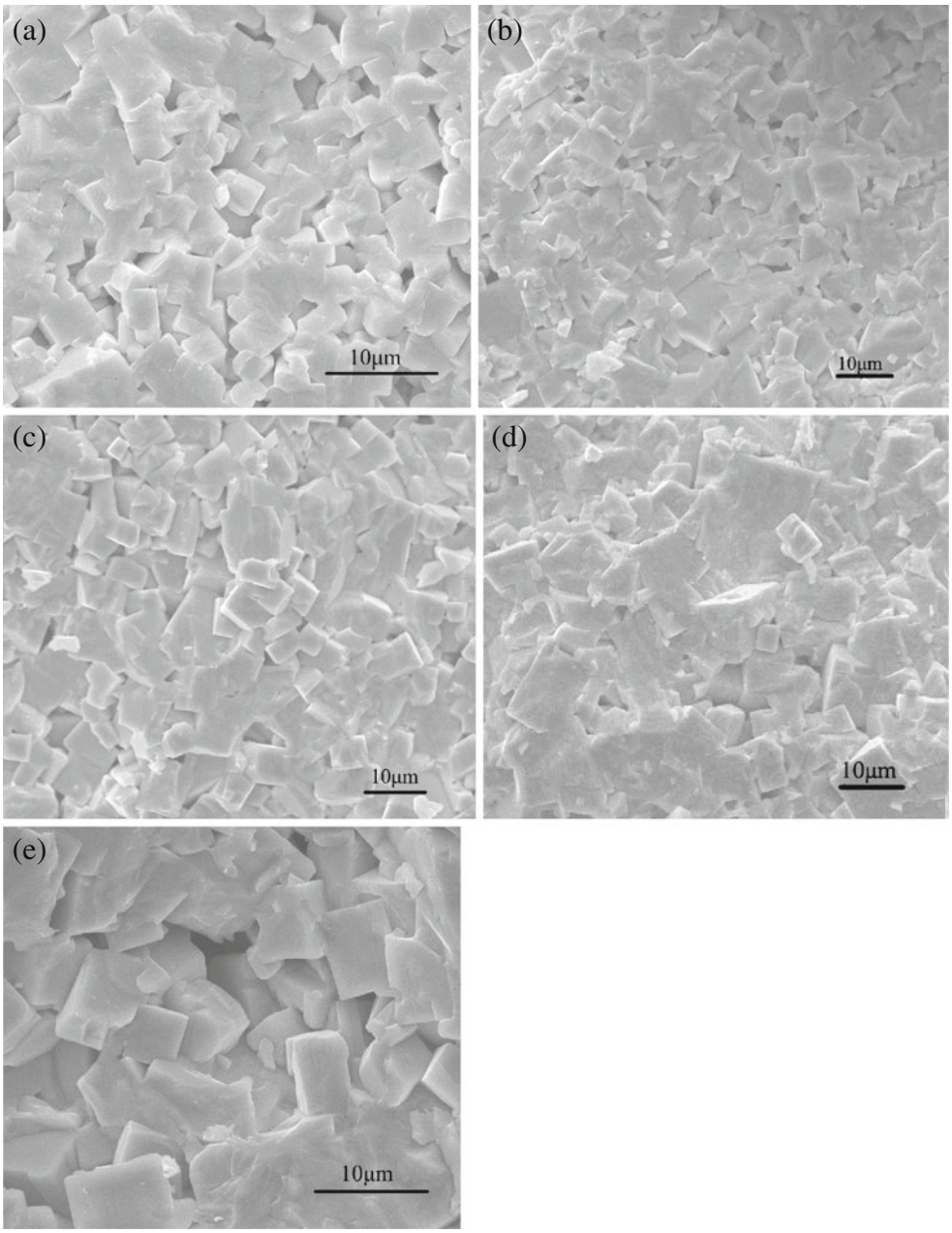

Fig. 4 SEM micrographs of fractured $0.94(K_{05}Na_{0.5})NbO_3$–$0.03LiNbO_3$–$0.03LiSbO_3$ ceramics sintered at (**a**) 1040°C (**b**) 1060°C, (**c**) 1080°C, (**d**) 1100°C (**e**) 1110°C for 2 h

(ZJ-3A, China). The temperature dependence on dielectric constant was investigated using LCR meter (ZL-10, China) in the range of 30–500°C at 1 kHz. A conventional Sawyer–Tower circuit was used to measure the polarization hysteresis (P–E) loop at 100 Hz.

3 Results and discussion

XRD patterns of the calcined powders and the crushed ceramic powders are shown in Fig. 2. It can be seen that the predominated phase of the calcined powders sintered at 850°C is orthorhombic phase which is characterized by (202)/(020) peak splitting about 45°, and a $LiSbO_3$ phase (ICDD: 43–0128) is detected as a secondary phase. Li_2CO_3 has a low melting point of 720°C and Sb_2O_3 also has a low melting point of 655°C. When calcined at 850°C, they exist as liquids [16]. As a result, the $LiSbO_3$ phase can be detected as a second phase. Figure 2 also shows XRD patterns of the crushed ceramic powders sintered at different temperatures. It can be concluded that the phase structure of all the crushed ceramic powders are tetragonal phase characterized by (002)/(200) peak splitting about 45°. The $LiSbO_3$ phase formed in calcined powders is not found in the crushed ceramic powders, indicating that $LiSbO_3$ has completely diffused into the NKN lattice to form a new

Table 2 The piezoelectric and dielectric properties of 0.94 $(K_{05}Na_{0.5})NbO_3$–0.03LiN-bO_3–0.03$LiSbO_3$ ceramics sintered at different temperatures

Sintering temperature (°C)	1040	1060	1080	1090	1100	1110
Loss tangent, tanδ	0.093	0.082	0.049	0.050	0.074	0.124
Dielectric permittivity, ε_r (1 kHz)	677	793	826	829	515	336
Planar coupling factor, k_p	0.31	0.29	0.30	0.30	0.30	0.23
Piezoelectric coefficient, d_{33} (pC/N)	152	174	190	176	165	140

solid solution. Although KNN, $LiNbO_3$ and $LiSbO_3$ have octahedral basic structure units (NbO_6 and SbO_6), their structures are different. KNN has the perovskite structure with space group *Amm*2 (C_{2v}^{14}), but $LiNbO_3$ and $LiSbO_3$ have lithium niobate structure, which could be described as heavily distorted perovskite or an ordered phase derived from the corundum structure with space group R_{3c} (C_{3v}^{6}) [16, 19]. As increasing the sintering temperature, Li^+ (0.92 Å, ionic diameter) could substitute for Na^+ (1.39 Å) and K^+ (1.64 Å), while Sb^{5+} (0.60 Å) could substitute for Nb^{5+} (0.69 Å). A complete solid solution with pure perovskite phase was formed at 1080°C. However, a $K_3Li_2Nb_5O_{15}$ (ICDD: 34–0122) phase with a tetragonal tungsten bronze structure begins to appear in crushed ceramic powders sintered at T>1080°C. It can be explained that the evaporation of potassium and sodium changes the stoichiometry of KNLNS ceramics and leads to the formation of the secondary phase. In addition, the diffraction peaks of crushed ceramic powders slightly shift toward a higher angle with the increase of the sintering temperature, which indicates shrinkage of the cell.

Figure 3 shows the density of ceramics as a function of the sintering temperature. It can be seen that the density firstly increases and then decreases with increasing temperature. The density of the KNLNS ceramics decreases as sintering temperature exceeds 1080°C, which may be due to the presence of $K_3Li_2Nb_5O_{15}$ phase with the lower density (theoretical density 4.38 g/cm^3). The highest density of 4.29 g/cm^3 (approaching to 95% of the theoretical density) is obtained at 1080°C. The result indicates that high densification is obtained by normal sintering for KNLNS ceramics and the optimum sintering temperature is 1080°C.

SEM micrographs of the fracture surface of KNLNS ceramics sintered at different temperatures are shown in Fig. 4. All the samples exhibit transgranular fracture with cubic shaped grains, which indicates that the grains are mechanically weaker than the grain boundaries. The grain sizes of the KNLNS ceramics become larger with the increase of sintering temperature. The average grain size of sintered NKNLS ceramics are approximately 2, 3, 5, 6, 8 μm for the samples sintered at 1040, 1060, 1080 and 1110°C, respectively. It can be explained according to the phenomenological kinetic grain growth equation expressed as follows

$$\log G = \frac{1}{n}\log t + \frac{1}{n}\left[\log K_0 - 0.434\frac{Q}{RT}\right]$$

where G is the average grain size at the time, n is the kinetic grain growth exponent, K_0 is a constant, Q is the apparent activation energy, R is the gas constant, and T is the absolute temperature [20]. As shown in Fig. 4(a), there are

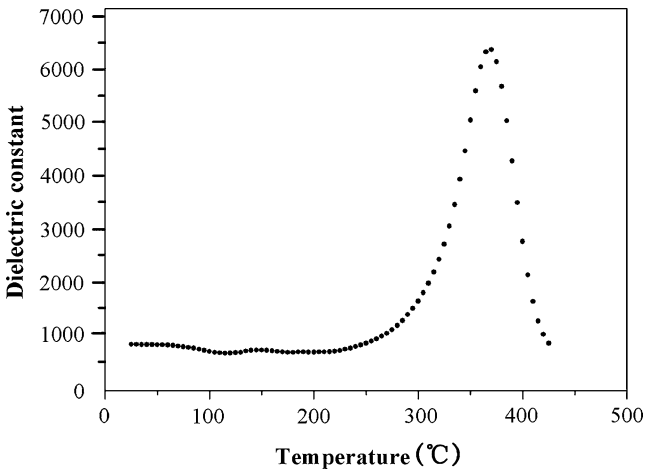

Fig. 5 The temperature dependence of relative dielectric constant ε_r (at 1 kHz) for the 0.94$(K_{05}Na_{0.5})NbO_3$–0.03$LiNbO_3$–0.03$LiSbO_3$ ceramics sintered at 1080°C

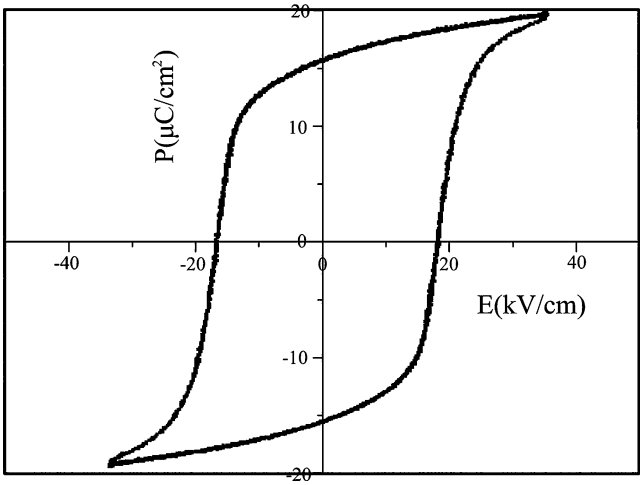

Fig. 6 P–E hysteresis of 0.94$(K_{05}Na_{0.5})NbO_3$–0.03$LiNbO_3$–0.03-$LiSbO_3$ ceramics

a number of pores and the grain sizes vary considerably. When the sintering temperature reaches 1080°C, a pore-less and dense structure can be seen in Fig. 4(b). The microstructure is much uniform and fine, and the grain boundary is very clear. When the sintering temperature is 1040°C (Fig. 4(a)), the grain has the angular shape with the flat surface, which is typically observed in the microstructure with abnormal grain growth (AGG). It is generally agreed that AGG is caused by the existence of a liquid phase [21–23]. Zhen *et al.* [23] found that extensive AGG occurred on the $(Li_{0.04}K_{0.44}Na_{0.52})NbO_3$ and $(Li_{0.04}K_{0.44}Na_{0.52})(Nb_{0.85}Ta_{0.15})O_3$ ceramics and concluded that the volatilization of alkali components was responsible for the occurrence of AGG. As shown in Fig. 4, it can be seen that the sample had several angular grains, whereas the grain sizes are still uniformly small, which proved that the formation of the liquid phase in ceramics. Therefore, the appearance of AGG may be ascribed to the low melting point of $K_3Li_2Nb_5O_{15}$ (melting point 1020°C), which was formed due to the volatilization of alkali components during sintering process at high temperature.

The piezoelectric constant (d_{33}), planar electromechanical coupling factor (k_p), relative dielectric constant (ε_r) and dielectric loss (tanδ) of samples as a function of sintering temperature are shown in Table 2. As the sintering temperature increases, d_{33} value of the samples increases at first and reaches the maximum of 190 pC/N at 1080°C. It is reported that grain size and density are most important factors for d_{33} [24]. This promotion may be attributed to the increase of density and grain size. The d_{33} value decreases when the sintering temperature exceeds 1080°C which can be attributed to the low density and the presence of $K_3Li_2Nb_5O_{15}$ phase. The ε_r value demonstrates the same trend as d_{33}. The largest value of 829 was obtained at 1090°C. The enhancement of ε_r is ascribed to the grain size increases which leads to a reduction of the grain boundary number [25]. The decreasing ε_r also could be due to the presence of the $K_3Li_2Nb_5O_{15}$ phase at 1100°C. The variation of tan δ with sintering temperature is opposite to those of d_{33}. At 1080°C, tanδ reaches its minimum of 0.049 which is related to the fine grains and the maximum density of KNLNS ceramics. The k_p changes little with the sintering temperature between 1080–1100°C, and then decreases greatly when the temperature exceeds 1100°C. As seen from Table 1, the density of our samples is a little bit lower than other NKN-based piezoelectric ceramics. Density and composition are the major factors to the piezoelectric properties (d_{33}, k_p). The composition of our samples is also different from other reports published in the literature. Different composition shows different piezoelectric properties. Therefore, the piezoelectric properties presented in our study are a little bit lower than those reported in other publications.

Figure 5 shows the temperature dependence of relative dielectric constant ε_r (at 1 kHz) for the KNLNS ceramics sintered at 1080°C. For pure NKN, phase transitions are observed at 420°C and 200°C, corresponding to the phase transitions of cubic–orthorhombic (at T_C) and orthorhombic–tetragonal (at T_{O-T}), respectively [19]. For samples sintered at 1080°C, only the cubic–orthorhombic phase transition was observed at 370°C which meant that the structure had changed from orthorhombic to tetragonal. This is consistent with the results of XRD analysis as discussed in Fig. 2. Dunmin Lin *et al.* also obtained similar results [26].

In order to characterize the ferroelectricity, P–E hysteresis loops of NKNLS ceramics are shown in Fig. 6. The remanent polarization (Pr) is 16.1 μC/cm^2 and the coercive electric field (Ec) is 17.6 kV/cm for KNNLS ceramics sintered at 1080°C. The saturated P–E hysteresis loops with high remnant polarization confirm the good ferroelectric nature of KNNLS ceramics.

4 Conclusions

The $0.94(K_{05}Na_{0.5})NbO_3$−$0.03LiNbO_3$−$0.03LiSbO_3$ piezoelectric ceramics were successfully fabricated by conventional mixed oxide route with normal sintering. As increasing sintering temperature, the density and electric properties were improved. A complete perovskite phase with tetragonal structure was formed at 1080°C. However, as the sintering temperature exceeded 1080°C, a $K_3Li_2Nb_5O_{15}$ phase with tetragonal tungsten bronze structure began to appear, the density and electric properties became deteriorated. A relatively homogeneous microstructure with fine grains, high density, and significantly enhanced electric properties were obtained at 1080°C.

Acknowledgements This work was supported by the Science and Technology Development Plan of Jinan (grant No. 046039).

References

1. T. Abraham, Am Ceram Bull **9**, 45–47 (2000)
2. T. Tani, T. Kimury, Adv Appl Ceram **105**, 55–65 (2006)
3. E. Cros, Nature **432**, 24–25 (2004)
4. G. Shirane, R. Newnham, R. Pepinsky, Phys Rev **96**, 581–588 (1954)
5. L. Egerton, D.M. Dillon, J Am Ceram Soc **42**, 438–442 (1959)
6. R.E. Jaeger, L. Egerton, J Am Ceram Soc **45**, 209–213 (1962)
7. G.H. Haertling, J Am Ceram Soc **50**, 329–330 (1967)
8. L. Egerton, C.A. Bieling, Ceram Bull **47**, 1151–1156 (1968)
9. J.F. Li, K. Wang, B.P. Zhang, L.M. Zhang, J Am Ceram Soc **89**, 706–709 (2006)
10. E. Ringgaard, T. Wurlitzer, J Eur Ceram Soc **25**, 2701–2706 (2005)

11. Y.P. Guo, K. Kakimoto, H. Ohsato, Solid State Commun **129**, 279–284 (2004)
12. Y.P. Guo, K. Kakimoto, H. Ohsato, Jpn J Appl Phys **43**, 6662–6666 (2004)
13. R.C. Chang, S.Y. Chu, Y.F. Lin, C.S. Hong, P.C. Kao, C.H. Lu, Sens Actuators A **138**, 355–360 (2007)
14. H.L. Du, F.S. Tang, D.J. Liu, W.C. Zhou, S.B. Qu, Mater Sci Eng B **136**, 165–169 (2007)
15. Y.P. Guo, K. Kakimoto, H. Ohsato, Mater Lett **59**, 241–244 (2005)
16. Z.P. Yang, Y.F. Chang, B. Liu, L.L. Wei, Mater Sci Eng A **432**, 292–298 (2006)
17. E. Hollenstein, M. Davis, D. Damjanovic, N. Setter, Appl Phys Lett **87**, 182905 (2005)
18. Y. Saito, H. Takao, T. Tani, T. Nonoyama, K. Takatori, T. Homma, T. Nagaya, M. Nakamura, Nature **432**, 84–87 (2004)
19. Y. Guo, K. Kakimoto, H. Ohsato, Appl Phys Lett **85**, 4121–4123 (2004)
20. T.Y. Chen, S.Y. Chu, Y.D. Juang, Sens Actuator A Phys **102**, 6–10 (2002)
21. J.S. Chun, N.M. Hwang, D.Y. Kim, J.K. Park, J Am Ceram Soc **87**, 1779–1781 (2004)
22. J.G. Fisher, B.K. Lee, A. Brancquart, J Eur Ceram Soc **25**, 2033–2036 (2005)
23. Y.H. Zhen, J.F. Li, J Am Ceram Soc **89**, 3669–3675 (2006)
24. K.H. Cho, H.Y. Park, C.W. Ahn, S. Nahm, J Am Ceram Soc **90**, 1946–1949 (2007)
25. H.L. Du, F.S. Tang, F. Luo, D.M. Zhu, S.B. Qu, Z.B. Pei, W.C. Zhou, Mater Res Bull **42**, 1594–1601 (2007)
26. D.M. Lin, K. Kwok, K. Lam, H. Chan, J Phys D Appl Phys **40**, 3500–3505 (2007)